REVIEW SUMMARY

NANOMATERIALS

High-entropy nanoparticles: Synthesis-structure-property relationships and data-driven discovery

Yonggang Yao†, Qi Dong†, Alexandra Brozena, Jian Luo, Jianwei Miao, Miaofang Chi, Chao Wang, Ioannis G. Kevrekidis, Zhiyong Jason Ren, Jeffrey Greeley, Guofeng Wang, Abraham Anapolsky, Liangbing Hu*

BACKGROUND: High-entropy nanoparticles contain more than four elements uniformly mixed into a solid-solution structure, offering opportunities for materials discovery, property optimization, and advanced applications. For example, the compositional flexibility of high-entropy nanoparticles enables fine-tuning of the catalytic activity and selectivity, and high-entropy mixing offers structural stability under harsh operating conditions. In addition, the multielemental synergy in high-entropy nanoparticles provides a diverse range of adsorption sites, which is ideal for multistep tandem reactions or reactions that require multifunctional catalysts. However, the wide range of possible compositions and complex atomic arrangements also create grand challenges in synthesizing, characterizing, understanding, and applying high-entropy nanoparticles. For example, controllable synthesis is challenging given the different physicochemical properties within the multielemental compositions combined with the small size and large surface area. Moreover, random multielemental mixing can make it difficult to precisely characterize the individual nanoparticles and their statistical variations. Without rational understanding and guidance, efficient compositional design and performance optimization within the huge multielemental space is nearly impossible.

ADVANCES: The comprehensive study of high-entropy nanoparticles has become feasible because of the rapid development of synthetic approaches, high-resolution characterization, high-throughput experimentation, and data-driven discovery. A diverse range of compositions and material libraries have been developed, many by using nonequilibrium "shock"–based methods designed to induce single-phase mixing even for traditionally immiscible elemental combinations. The nanomaterial types have also rapidly evolved from crystalline metallic alloys to metallic glasses, oxides, sulfides, phosphates, and others. Advanced characterization tools have been used to uncover the structural complexities of high-entropy nanoparticles. For example, atomic electron tomography has been used for single-atom-level resolution of the three-dimensional positions of the elements and their chemical environments. Finally, high-entropy nanoparticles have already shown promise in a wide range of catalysis and energy technologies because of their atomic structure and tunable electronic states. The development of high-throughput computational and experimental methods can accelerate the material exploration rate and enable machine-learning tools that are ideal for performance prediction and guided optimization. Materials discovery platforms, such as high-throughput exploration and data mining, may disruptively supplant conventional trial-and-error approaches for developing next-generation catalysts based on high-entropy nanoparticles.

OUTLOOK: High-entropy nanoparticles provide an enticing material platform for different applications. Being at an initial stage, enormous opportunities and grand challenges exist for these intrinsically complex materials. For the next stage of research and applications, we need (i) the controlled synthesis of high-entropy nanoparticles with targeted surface compositions and atomic arrangements; (ii) fundamental studies of surfaces, ordering, defects, and the dynamic evolution of high-entropy nanoparticles under catalytic conditions through precise structural characterization; (iii) identification and understanding of the active sites and performance origin (especially the enhanced stability) of high-entropy nanoparticles; and (iv) high-throughput computational and experimental techniques for rapid screening and data mining toward accelerated exploration of high-entropy nanoparticles in a multielemental space. We expect that discoveries about the synthesis-structure-property relationships of high-entropy nanoparticles and their guided discovery will greatly benefit a range of applications for catalysis, energy, and sustainability. ■

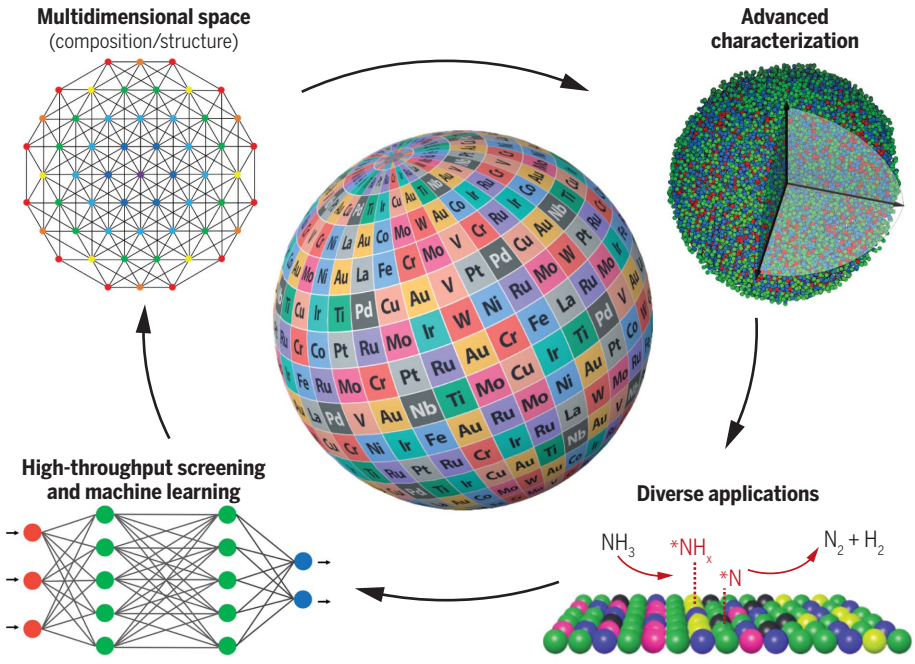

High-entropy nanoparticles and data-driven discovery. Emerging high-entropy nanoparticles feature multielemental mixing within a large compositional space and can be used for diverse applications, particularly for catalysis. High-throughput and machine-learning tools, coupled with advanced characterization techniques, can substantially accelerate the optimization of these high-entropy nanoparticles, forming a closed-loop paradigm toward data-driven discovery.

CREDITS: TOP RIGHT: YANG *ET AL.*, *NATURE* **592**, 60–64 (2021); CENTER: JIAQI DAI; BOTTOM RIGHT: XIE *ET AL.*, *NAT. COMMUN.***10**, 4011 (2019)

The list of author affiliations is available in the full article online.
*Corresponding author. Email: binghu@umd.edu
†These authors contributed equally to this work.
Cite this article as Y. Yao *et al.*, *Science* **376**, eabn3103 (2022). DOI: 10.1126/science.abn3103

REVIEW

NANOMATERIALS

High-entropy nanoparticles: Synthesis-structure-property relationships and data-driven discovery

Yonggang Yao[1]†, Qi Dong[1]†, Alexandra Brozena[1], Jian Luo[2], Jianwei Miao[3], Miaofang Chi[4], Chao Wang[5], Ioannis G. Kevrekidis[5], Zhiyong Jason Ren[6], Jeffrey Greeley[7], Guofeng Wang[8], Abraham Anapolsky[9], Liangbing Hu[1,10]*

High-entropy nanoparticles have become a rapidly growing area of research in recent years. Because of their multielemental compositions and unique high-entropy mixing states (i.e., solid-solution) that can lead to tunable activity and enhanced stability, these nanoparticles have received notable attention for catalyst design and exploration. However, this strong potential is also accompanied by grand challenges originating from their vast compositional space and complex atomic structure, which hinder comprehensive exploration and fundamental understanding. Through a multidisciplinary view of synthesis, characterization, catalytic applications, high-throughput screening, and data-driven materials discovery, this review is dedicated to discussing the important progress of high-entropy nanoparticles and unveiling the critical needs for their future development for catalysis, energy, and sustainability applications.

High-entropy nanoparticles have received a great amount of attention in recent years because of their multielemental composition (typically five or more elements) and homogeneously mixed solid-solution state, providing not only an enormous number of combinations for materials discovery but also a unique microstructure for property optimization (Fig. 1A) (*1*–*3*). Early reports of multielemental (five or more) alloy nanoparticles suggested the potential of these unique materials (*4*–*6*) but did not provide detailed structural understanding or reveal a general synthesis route for different compositions. In 2016, Mirkin and colleagues made a substantial advance in synthesizing various compositions of multielemental nanoparticles using confined nanoreactors (*7*). However, these materials featured heterogeneous structures with phase separation due to elemental immiscibility. Recent advances in ultrafast synthetic methodologies, such as nonequilibrium thermal-shock-based approaches, have since enabled a variety of high-entropy nanoparticles without phase separation, even among immiscible elemental combinations (Fig. 1B) (*8*). In a typical thermal shock process (e.g., 2000 K in 55 ms), the rapid heating of precursors to a high temperature induces multielemental mixing and alloying to achieve a solid-solution state, whereas the short heating duration and subsequent rapid quenching help to retain and freeze the uniform structure and small particle size (*8*). Since then, various high-entropy nanomaterials, including alloys (e.g., PtPdFeCoNiAuCuSn) (*9*–*14*), metallic glasses (e.g., amorphous CoCrMnNiV) (*15*, *16*), intermetallics [e.g., $L1_0$ type $(Pt_{0.8}Pd_{0.1}Au_{0.1})(Fe_{0.6}Co_{0.1}Ni_{i0.1}Cu_{0.1}Sn_{0.1})$] (*17*, *18*), oxides, fluorides, sulfides, carbides, MXenes (*19*–*25*), and van der Waals materials (e.g., dichalcogenides, halides, and phosphorus trisulfide) (*26*), have all been successfully demonstrated using thermal shock and other nonequilibrium approaches.

Despite having been developed only recently, high-entropy nanoparticles have already shown great promise for a range of emerging energy-related processes and applications, particularly in catalysis (Fig. 1C) (*27*–*36*). The compositional flexibility of high-entropy nanoparticles enables fine-tuning of the catalytic activity, whereas the high-entropy solid-solution mixing potentially offers structural stability 1that is critical for operation under harsh conditions. For example, non-noble $(Co_xMo_{0.7-x})Fe_{0.1}Ni_{0.1}Cu_{0.1}$ nanoparticles have been shown to overcome the immiscibility of Co–Mo, allowing for robust tuning of the Co–Mo ratios and associated surface adsorption properties. As a result, $(Co_{0.25}Mo_{0.45})Fe_{0.1}Ni_{0.1}Cu_{0.1}$ nanoparticles have demonstrated a fourfold improvement in ammonia decomposition compared with noble Ru and are stable at 500°C for 50 hours without noticeable degradation (*36*). In another example, $Pt_{18}Ni_{26}Fe_{15}Co_{14}Cu_{27}$ nanoparticles were developed for electrochemical hydrogen evolution and showed a lower onset potential (11 versus 84 mV), a higher activity (10.98 versus 0.83 A/mg_{Pt}), and excellent stability compared with commercial Pt–C catalysts (*11*). These examples epitomize the strong potential of high-entropy nanoparticles as highly efficient and cost-effective catalysts (*9*, *11*, *12*, *20*, *36*–*39*).

Compared with materials having relatively simple compositions (i.e., one to three elements), high-entropy nanoparticles have two distinct features: (i) a vast compositional space that derives from the multielemental combinations and (ii) complex atomic configurations due to the random multielemental mixing. The former provides huge compositional choices for catalyst design and development, and the latter makes these materials fundamentally different from conventional catalysts in that they feature a diverse range of adsorption sites and a near-continuous binding energy distribution pattern (*40*, *41*). These qualities are particularly attractive for complex or tandem reactions that involve numerous intermediate steps and require multifunctionality (*28*, *38*, *40*, *42*–*44*).

However, along with these opportunities, the vast number of possible compositions and complex atomic arrangements create grand challenges in the design, synthesis, characterization, and application of these unique nanomaterials. First, considering the wide span of physicochemical properties (e.g., atomic size and electronic structure) among the different constituent elements, synthesizing high-entropy nanoparticles in a highly controllable manner is difficult. Moreover, characterizing the detailed structure of high-entropy nanoparticles, such as the reactive surfaces and defects, is challenging or still lacking because of the complex atomic configurations and multiple elements of similar electron contrasts. Additionally, we have very limited knowledge of how elemental composition and synthesis methods affect the structure and properties of high-entropy nanoparticles. Although identifying these relationships for such complex materials is a daunting task, understanding them is critical to guiding material design and optimization.

In response to the increasing interest, rapid development, and large challenges of this field, we aim to highlight the important progress and critical unknowns regarding the synthesis, structure, characterization, and applications of high-entropy nanoparticles. We also discuss the potential and implementation of computationally guided and data-driven

[1]Department of Materials Science and Engineering, University of Maryland, College Park, MD 20742, USA. [2]Department of NanoEngineering, Program of Materials Science and Engineering, University of California San Diego, La Jolla, CA 92093, USA. [3]Department of Physics and Astronomy and California NanoSystems Institute, University of California, Los Angeles, Los Angeles, CA 90095, USA. [4]Center for Nanophase Materials Sciences, Oak Ridge National Laboratory, Oak Ridge, TN 37932, USA. [5]Department of Chemical and Biomolecular Engineering, Johns Hopkins University, Baltimore, MD 21218, USA. [6]Department of Civil and Environmental Engineering and Andlinger Center for Energy and the Environment, Princeton University, Princeton, NJ 08544, USA. [7]School of Chemical Engineering, Purdue University, West Lafayette, IN 47907, USA. [8]Department of Mechanical Engineering and Materials Science, University of Pittsburgh, Pittsburgh, PA 15261, USA. [9]Toyota Research Institute, Los Altos, CA 94022, USA. [10]Center for Materials Innovation, University of Maryland, College Park, MD 20742, USA.
*Corresponding author. Email: binghu@umd.edu
†These authors contributed equally to this work.

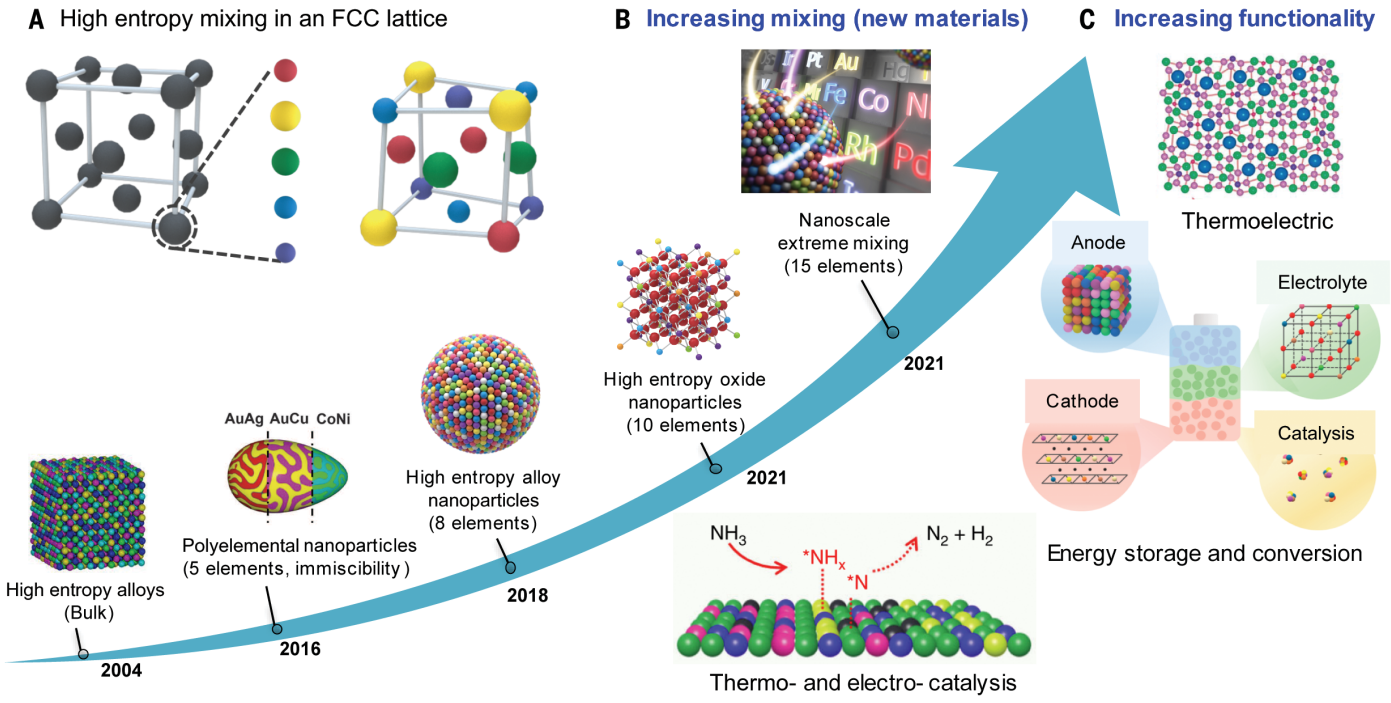

Fig. 1. Development of high-entropy nanoparticles with multielemental composition and enhanced functionality. (**A**) Schematic showing high-entropy mixing in a face-centered cubic lattice. Multiple elements will occupy the same lattice site randomly to form a high-entropy structure such as a high-entropy alloy. (**B**) The study of bulk high-entropy alloys has taken off and gained substantial interests since 2004 (*1*, *3*). In 2016, a multielemental nanoparticle library was synthesized (though with immiscibility, and thus phase segregation), followed by various single-phase, high-entropy nanoparticles with an increasing number and range of elements (*7*, *8*, *14*, *20*). Reprinted from (*14*) with permission from Elsevier. (**C**) These high-entropy nanoparticles have found critical application in thermo- and electro-catalysis, energy storage and conversation, and environmental and thermoelectric technologies (*29*–*31*, *35*, *36*). Reprinted from (*31*) with permission (copyright 2021 American Chemical Society) and from (*35*) with permission. Other portions of the figure are reprinted from (*7*, *8*) with permission, from (*20*) with permission from Springer-Nature, and from (*36*) CC BY 4.0.

accelerated exploration of high-entropy nanoparticles, along with the remaining challenges and future directions for this field. We intend to stimulate continuing and integrated efforts from multiple disciplines to study high-entropy nanoparticles and explore synthesis-structure-property relationships in the multidimensional space. Note that we use the term "high-entropy nanoparticles" to refer to such particles with a complex composition (five or more elements) and solid-solution structure rather than the conventional definition based on the somewhat subjective threshold of 1.5 k_B per atom for metals or per cation for ceramics, where k_B is the Boltzmann constant (*3*, *45*). In this review, although we focus on high-entropy nanoparticles, the basic concepts are expected to be applicable to other nanomaterials as well. We anticipate that with these advances, high-entropy nanoparticles will have a substantial impact in many fields and particularly catalysis, where this new material can potentially replace the longstanding noble metal counterparts.

High-entropy nanoparticle synthesis

From a thermodynamic point of view, the formation of high-entropy nanoparticles is a result of competition between enthalpy and entropy ($\Delta G = \Delta H - T \bullet \Delta S$). The configurational entropy of high-entropy nanoparticles increases with a greater number of elements and acts as a driving force for single-phase mixing (Fig. 2A). The enthalpy of the multielemental interactions (ΔH_{ij}) varies largely depending on the nature of the constituent elements, which directly affects the resulting phase under near-equilibrium conditions (Fig. 2B). For example, elemental combinations that have highly positive values of ΔH_{ij} (i.e., repelling force) cause immiscibility and phase segregation, whereas highly negative values of ΔH_{ij} (i.e., attractive force) promote structural ordering, such as intermetallic formation. If all ΔH_{ij} pairs in the multielement composition are near-zero values, indicating little attraction or repelling between these elements, the entropic term then dominates and promotes homogeneous random elemental mixing and high-entropy formation (Fig. 2B). However, because of the large physicochemical differences among different elements (i.e., the wide range of ΔH_{ij} values), natural single-phase mixing is often challenging and rare (*46*, *47*), with phase-segregated structures being more typical when using near-equilibrium approaches (e.g., wet chemistry) to synthesize multielemental nanoparticles (*7*, *48*, *49*).

The initial breakthrough in the general synthesis of high-entropy alloy (HEA) nanoparticles with a wide compositional range (including many immiscible combinations) and large elemental numbers (up to eight) was realized by a high-temperature "thermal shock" process invented by the Hu group at the University of Maryland (*8*, *50*–*52*) (Fig. 2C). The cooling rate of this synthesis approach is an important parameter because it affects the degree of nonequilibrium and structural ordering that can be achieved by the constituent elements, as described in the well-known temperature-time-transformation diagrams used in physical metallurgy and polymer curing (Fig. 2D) (*8*, *53*, *54*). The generated structures can include metallic glass nanoparticles (random mixing in a disordered lattice), regular HEA nanoparticles (random mixing in a crystalline lattice), intermetallic nanoparticles (chemical ordering between sublattices but random mixing within each sublattice), and heterogeneous nanoparticles (phase separation) (*8*, *17*). Moreover, the short duration and rapid quenching of thermal shock synthesis also assist the formation of small and uniform particles (*8*, *55*), which can be further modulated through defect engineering and appropriate substrates (*56*–*58*). Similar to this "shock"-based concept, a variety

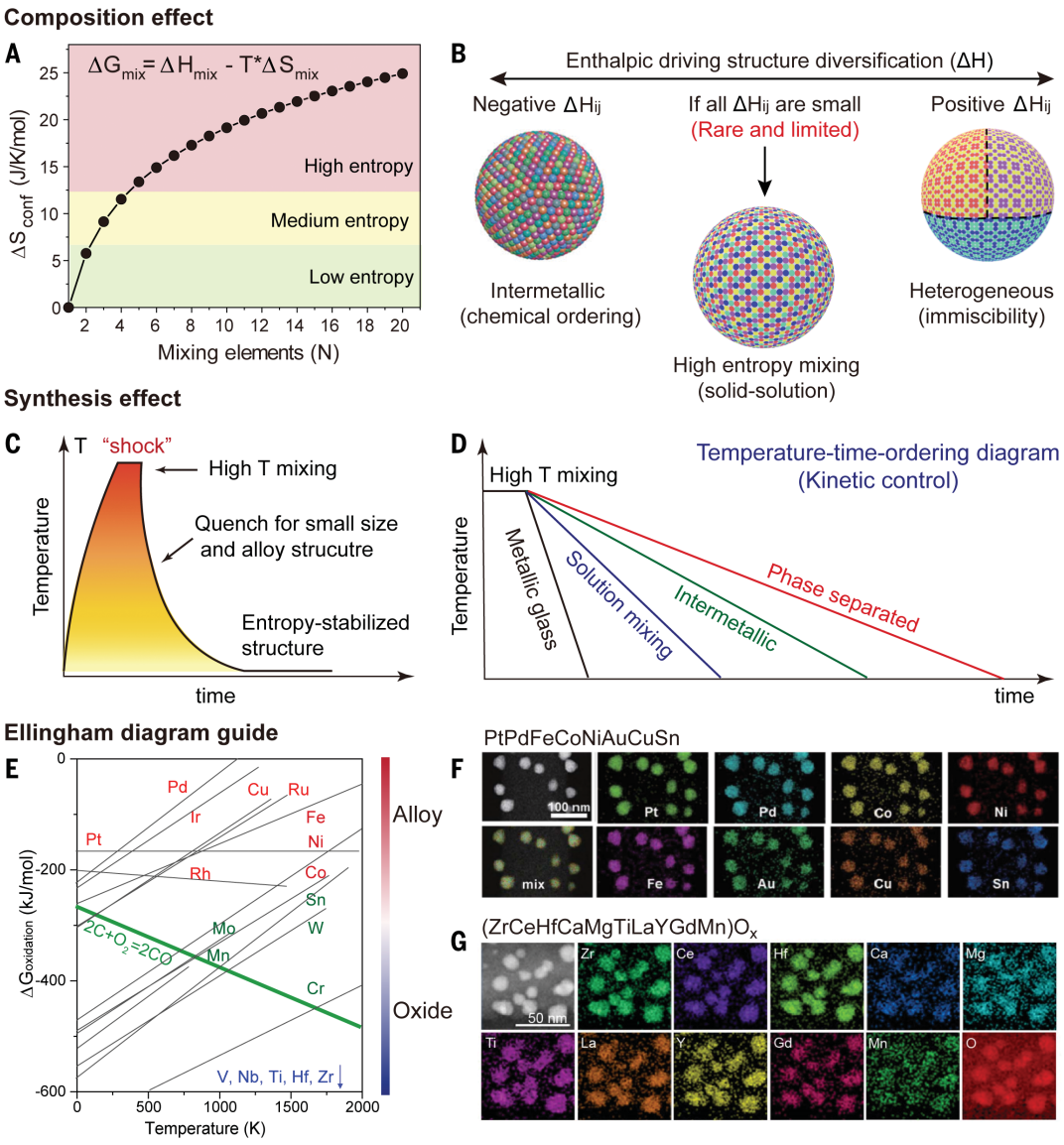

Fig. 2. High-entropy nanoparticle synthesis and structure. Thermodynamic analysis of high-entropy mixing considers both entropy (**A**) and enthalpy (**B**), which are mainly determined by the composition of high-entropy nanoparticles (*8*). (**C**) Thermal shock synthesis of high-entropy nanoparticles features a high-temperature pulse for elemental mixing and then rapid temperature quenching to maintain the high-entropy structure. (**D**) Temperature-time-transformation diagram describing how the cooling rates of high-temperature, kinetically controlled syntheses can be adjusted to form various nanoparticles featuring different degrees of structural and chemical ordering. (**E**) The Ellingham diagram [reprinted from (*14*) with permission from Elsevier] provides a guide for composing either alloy (e.g., PtPdFeCoNiAuCuSn) (*8*) (**F**) or oxide high-entropy nanoparticles (e.g., ZeCeHfCaMgTiLaYGdMnO_x) (*20*) (**G**) according to the oxidation potentials of each element. Reprinted from (*20*) with permission from Springer Nature.

of other methods have also been developed that have enabled a wide range of high-entropy nanoparticles, including vapor phase spark discharge (*13*), rapid radiative heating or annealing (*12*, *59*, *60*), acute chemical reduction (*33*, *43*), low-temperature hydrogen spillover (*61*), sputtering (*9*, *62*–*64*), transient electrosynthesis (*15*), and plasma, laser, and microwave heating (*65*–*67*), all featuring a strong kinetics-driven process. These rapid, shock-type syntheses are also fast enough to enable the efficient manufacturing of nanocatalysts (*10*, *12*, *13*, *68*, *69*).

The Ellingham diagram can be used to guide the thermochemical synthesis of high-entropy nanoparticles by illustrating the oxidation potential of the constituent elements as a function of temperature (Fig. 2E). Despite being initially developed for bulk metallurgy, we found that the Ellingham diagram is also applicable for nanoscale, shock-type reactions (*14*, *20*). Generally, elements closer to the top of the Ellingham diagram, such as noble metals and Fe, Co, and Cu, have smaller oxidation potentials (i.e., are more easily reduced) and can form alloy nanoparticles through high-temperature syntheses, such as octonary HEA nanoparticles of PtPdFeCoNiAuCuSn (Fig. 2F) (*8*). By contrast, elements near the bottom of the diagram, such as Zr, Ti, Hf, and Nb, have larger oxidation potentials and can form high-entropy oxide nanoparticles, such as (ZrCeHfCaMgTiLaYGdMn)O_x (Fig. 2G) (*20*). For the elements in the middle, such as Mo, W, and Mn (as shown in green in Fig. 2E) with moderate oxidation potentials, different synthesis strategies have been explored that can toggle the elements between their metallic and oxide states, thus expanding possible

high-entropy alloy or oxide elemental spaces (*14*, *20*, *70*). In addition to high-entropy oxides (*8*), other high-entropy compounds (e.g., sulfides and carbides) have also been synthesized with a wide range of sizes, shapes, and phases (*8*, *12*, *14*–*18*, *26*–*30*, *71*).

Advanced characterization

High-entropy nanoparticles should display a single-phase structure, demonstrating uniform and random mixing of the constituent elements. However, the characterization of this random mixing of multielements and their synergy is very challenging. Conventional techniques, such as powder x-ray diffraction (XRD, λ = 1.5418 Å), scanning and transmission electron microscopy (SEM and TEM, respectively), and x-ray photoelectron spectroscopy (XPS), can help to determine the basic phase structure, morphology, elemental distribution, and valence state, but may lack the required resolution to decouple the multielemental mixing. Synchrotron x-ray–based techniques, which use a much shorter wavelength (e.g., λ = 0.2113 Å), can provide a high resolution to better understand the atomic arrangement, bonding and coordination, and electronic properties of high-entropy nanoparticles (Fig. 3A). For example, synchrotron XRD can detect the overall phase structure

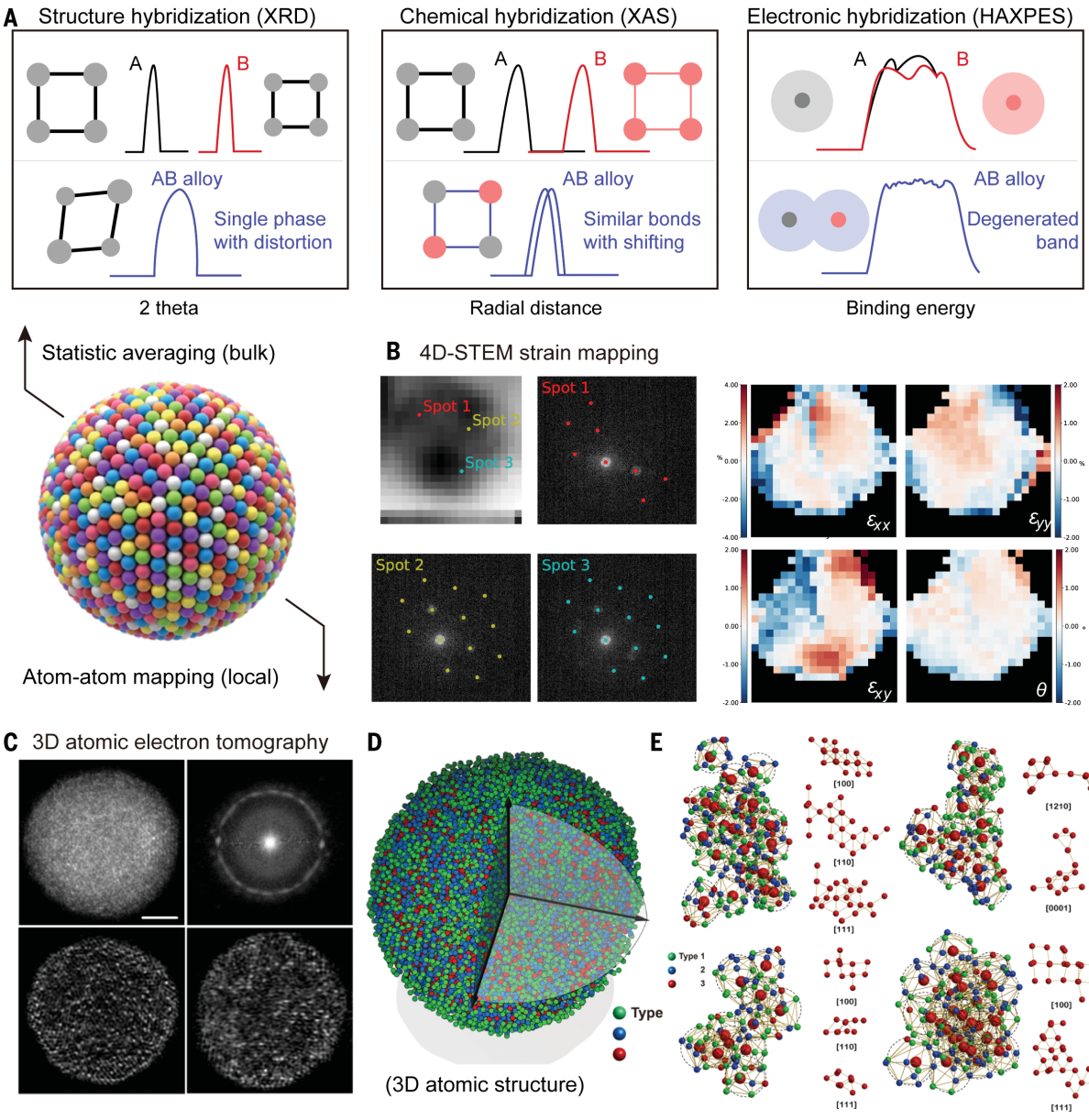

Fig. 3. Advanced characterization of high-entropy nanoparticles. (**A**) Schematic of the macroscopic and bulk characterization of the structural, chemical, and electronic hybridization in high-entropy nanoparticles through x-ray–based techniques, including XRD, XAS, and HAXPES, particularly using synchrotron x-ray sources that provide higher resolution. (**B**) 4D-STEM and strain mapping of a high-entropy nanoparticle, in which local diffraction (e.g., spots 1 to 3) is collected and compared with the average structure to derive the local lattice strain distribution including tensile (red) and compressive (blue). Reprinted from (*14*) with permission from Elsevier. (**C**) Determining the 3D atomic structure of a high-entropy metallic glass nanoparticle by AET. Shown are a representative experimental image (top left), the average 2D power spectrum (top right), and two 2.4-Å-thick slices of the 3D reconstruction in the *x*–*y* and *y*–*z* planes (bottom). Scale bar, 2 nm. (**D**) Experimental 3D atomic model of the high-entropy metallic glass nanoparticle. (**E**) Identification of four types of crystal-like medium-range order that coexist in the metallic glass nanoparticle based on AET results (*16*). Reprinted from (*8*) with permission and from (*36*) (CC BY 4.0).

as well as possible immiscible phases and impurities in high-entropy nanoparticles with greater accuracy (*49*, *72*), confirming whether high-entropy mixing is achieved. x-ray absorption spectroscopy (XAS) is an element-specific technique that can be used to study the atomic and/or local coordination environment of each element, which is critical to understanding the multielemental mixing and possible short-range or local ordering in high-entropy nanoparticles (*14*, *73*, *74*). Finally, hard x-ray photoelectron spectroscopy (HAXPES) can reveal the electronic structure (e.g., valence band and d-band center) in high-entropy nanoparticles, which is closely related to the adsorption and binding energy of key reaction intermediates, helping to rationalize the corresponding catalytic activity (*75*).

Although x-ray techniques can provide statistical analysis, electron microscopy–based techniques are critical to directly visualizing the particle size and distribution, phase, structure, composition, and chemical environments. For example, in situ TEM has been used to study nanoparticles synthesized by the high-temperature shock method, revealing the formation process as well as their dispersion and stability on defective carbon substrates (*76*). Another advanced approach that could meet higher-throughput and higher-resolution needs is four-dimensional scanning transmission electron microscopy (4D-STEM) (Fig. 3B) (*14*, *77*). 4D-STEM uses a small probe (~1 nm) to scan a large geometric region of up to ~1 × 1 μm^2 in area, thus enabling fast and high-resolution characterization of high-entropy nanoparticles for local lattice distortion, structural heterogeneity, and short-range ordering (*78*). As shown in Fig. 3B, local diffraction patterns can be obtained on high-entropy nanoparticles, and corresponding strain maps within the nanoparticles can be generated by comparing the differences between the local and average phase structures (*14*, *77*), indicating potential lattice distortion and strain.

For more advanced characterization of the 3D atomic structure, atomic electron tomography (AET) has proven to be the method of choice (Fig. 3C) (*79*–*81*). Very recently, AET was sufficiently advanced to resolve the 3D atomic structure of a high-entropy metallic glass nanoparticle containing eight elements: Co, Ni, Ru, Rh, Pd, Ag, Ir, and Pt (Fig. 3C) (*16*). Because the image contrast of AET depends on the atomic number, AET is currently only sensitive enough to classify the eight elements into three types: Co and Ni as type 1 (green); Ru, Rh, Pd, and Ag as type 2 (blue); and Ir and Pt as type 3 (red) (Fig. 3, D and E). Figure 3D shows the 3D atomic structure of the high-entropy metallic glass nanoparticle, in which the type 1, 2, and 3 atoms are uniformly distributed. The 3D atomic structure revealed four different crystal-like medium-range orderings, including face-centered cubic, hexagonal close-packed, body-centered cubic, and simple cubic structures that coexist in the high-entropy nanoparticle (Fig. 3E). These results provide direct experimental evidence that support the general framework of the efficient cluster packing model of metallic glasses (*82*) and demonstrate how AET techniques will enable researchers to study the 3D structure of high-entropy nanoparticles at the single-atom level.

Multifunctional catalytic activity

Previously, high-entropy materials, particularly high-entropy alloys, were mostly used for structural engineering applications (*3*). Wang *et al.* for the first time demonstrated that high-entropy alloy nanoparticles can serve as highly efficient catalysts in thermocatalysis (*8*, *36*). In catalysis, the binding of reactants or intermediates to the catalyst surface should be neither too strong nor too weak (the Sabatier principle) to maximize the performance, thus showing a "volcano plot" in the dependence of activity on binding energy (*83*, *84*). As schematically shown in Fig. 4A, the binding energy distribution patterns of individual elements (e.g., Co, Mo, Fe, Ni, and Cu) often exhibit sharp peaks because of their relatively fixed structure and adsorption sites. However, when multiple elements are mixed into high-entropy alloys (e.g., CoMoFeNiCu), their adsorption energy could transform into a broadened, multipeak, nearly continuous spectrum through electronic hybridization. Recently, Löffler *et al.* reported "current-wave" patterns in electrocatalysis on high-entropy catalysts, where multiple inflection points and current plateaus were observed, a strong indication of multiple active site centers in the high-entropy nanoparticles (*40*, *42*).

Because of the unique binding energy distribution, high-entropy nanoparticles can be readily tuned to obtain the desired surface properties for optimal catalytic performance (*28*, *40*, *62*). For example, in the NH_3 decomposition reaction ($2NH_3 \rightarrow N_2 + 3H_2$), it was theoretically proposed that non-noble Co–Mo alloy could outperform Ru because of the optimized *N adsorption based on the theoretical analysis (volcano plot in Fig. 4B) (*85*); however, such a design is hindered by the immiscibility between Co and Mo. Recently, alloyed CoMo-based catalysts were demonstrated in $(Co_xMo_{1-x})_{70}(FeNiCu)_{30}$ HEA nanoparticles synthesized using the thermal shock method (*36*). The Co:Mo elemental ratio can be tuned to optimize the nitrogen adsorption energy (ΔE_N) under the given reaction conditions, achieving superior performance compared with Ru, the most active monometallic catalyst (Fig. 4C). Similar high performances of high-entropy nanocatalysts have also been observed in many other systems (*9*, *15*, *20*, *43*, *62*, *73*, *75*, *86*, *87*), demonstrating the importance of multielemental design and compositional tunability. It should be noted that the diverse and heterogeneous active sites can lead to statistical variations in local activity (<50 nm) but overall repeatable performances (*88*).

Theoretically, the volcano plot can be interpreted as the result of the linear scaling relation (LSR) in first-principle calculation studies (*85*, *89*). The LSR says that in a complex or multistep reaction, the adsorption energies of reaction intermediates (e.g., O* or OH*) are linearly linked or scale linearly (*83*); in other words, strong adsorption of reactants will likely lead to the strong adsorption of products (i.e., difficult to desorb), thus slowing down the reaction substantially (*90*). Many strategies have been proposed to circumvent the LSR in nanoparticle catalyst design, including the introduction of co-adsorbates and tethers, promoters, ligands, and new alloys with complex synergy between the constituent elements (*83*, *85*). High-entropy nanoparticles offer complex atomic configurations, diverse adsorption sites, and tunable binding energies that could lead to a range of new opportunities compared with simple catalysts (*83*). For example, Wu *et al.* reported noble IrPdPtRhRu HEA nanoparticles for the hydrogen evolution reaction ($2H_2O \rightarrow O_2 + 2H_2$) and found that the material displayed superior performance compared with individual metals (Ir, Pd, Pt, Rh, and Ru) (Fig. 4D) (*75*). More importantly, the turnover frequency of the IrPdPtRhRu was far beyond what was expected by traditional LSR theories (blue region in Fig. 4E), suggesting the HEA's ability to circumvent the LSR predictions.

In addition, the broadband adsorption energy landscape of high-entropy nanoparticles is particularly promising for catalysis in tandem and complex reactions, which normally require different active sites and adsorption for multiple reaction intermediates to achieve overall high activity and/or selectivity (*27*, *71*). For example, in the ethanol oxidation reaction, which involves a complex 12-electron transfer and a range of intermediates, high-entropy PtPdRuRhOsIr (PGM-HEA) nanoparticles not only demonstrated a much higher activity than monometallic catalysts and their physical mixture but also enabled a much higher 12-electron selectivity to complete oxidation to CO_2 (Fig. 4F) (*43*, *62*, *71*). In another example, $Ru_{22}Fe_{20}Co_{18}Ni_{21}Cu_{19}$ HEA nanoparticles demonstrated high activity and selectivity in the nitrogen reduction reaction (NRR: $N_2 + 3H_2 \rightarrow 2NH_3$) (*38*). Theoretical analysis found that Fe in the HEA is suitable for N_2 adsorption and dissociation, whereas the nearby Co–Cu and Ru–Ni combinations favor H_2 adsorption and dissociation, illustrating the importance of multifunctional active sites for overall efficient NH_3 synthesis. Similarly, high-performance high-entropy nanoparticles have been reported for other complex

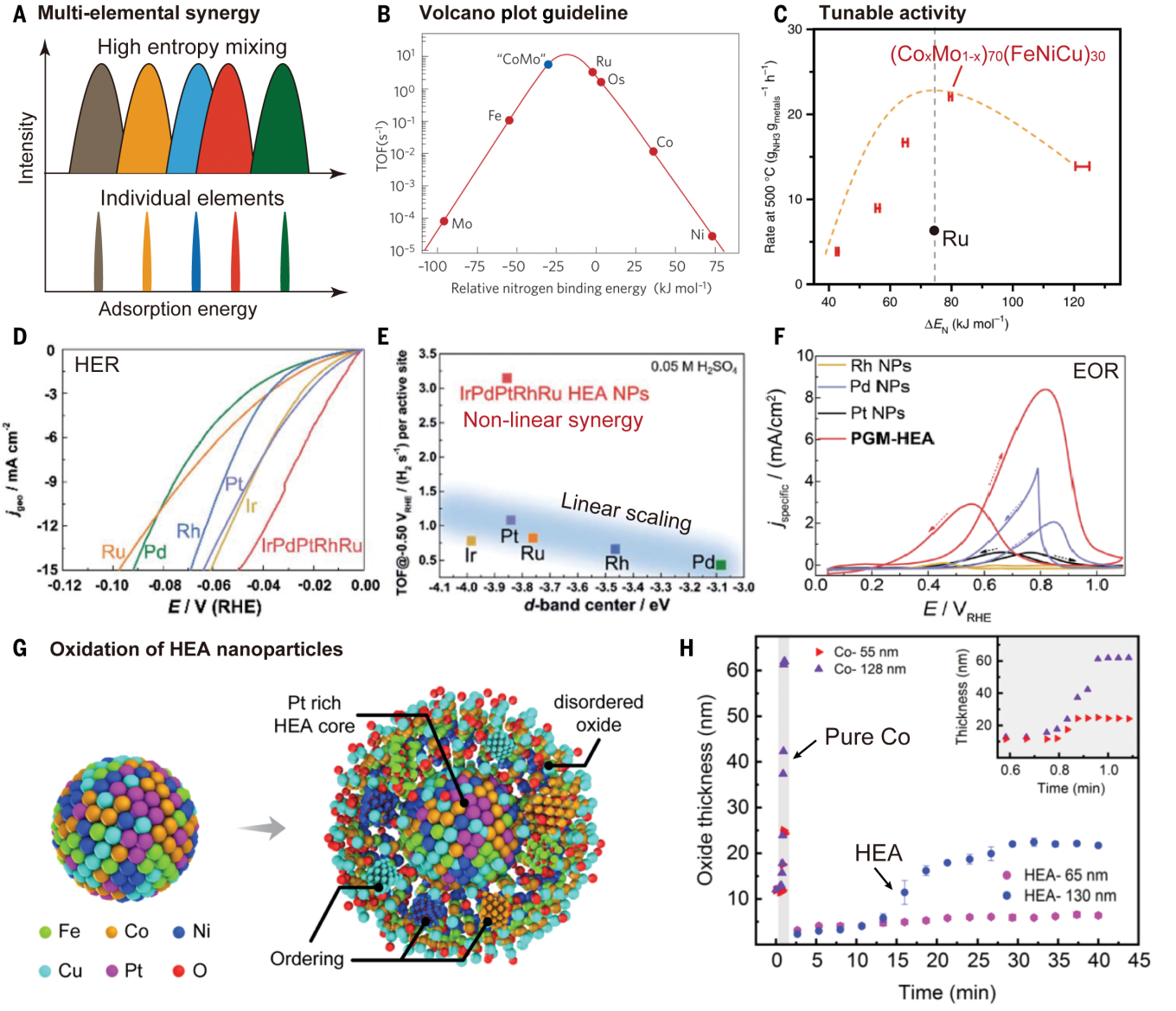

Fig. 4. High-entropy nanoparticles in catalytic reactions. (**A**) Multielemental synergy in high-entropy nanoparticles leads to multiactive sites and a broadband binding energy distribution pattern (*40*, *42*). (**B**) The composition volcano plot is a facile guide for designing high-performance catalysts, in which alloying can enable tuning of the adsorption energy toward peak performance, such as CoMo alloys. Reprinted from (*100*) with permission from Springer Nature. (**C**) Optimized CoMoFeNiCu HEA nanoparticles showed a four times higher conversion rate at 500°C compared with Ru, which was achieved by adjusting the composition ratio between Co and Mo to adjust the ΔE_N. Reprinted from (*36*) (CC BY 4.0). (**D** and **E**) IrPdPtRhRu HEA nanoparticles display superior hydrogen evolution reaction performance (D) and a much higher turnover frequency than that of the individual metals after a linear scaling relation (E), indicating strong nonlinear synergy in HEA catalysts. Reprinted from (*75*). (**F**) PGM-HEA (IrPdPtRhRuOs) nanoparticles show excellent performance for the complex and multistep ethanol oxidation reaction (EOR) compared with individual metals (*43*). (**G**) In situ oxidation of HEA nanoparticles (PtFeCoNiCu) leads to an HEA-core/oxide-shell structure. (**H**) HEA nanoparticles show much slower logarithmic oxidation kinetics compared with pure Co, which catastrophically oxidized in 1 min. Reprinted from (*97*) with permission (copyright 2021 American Chemical Society).

and multistep reactions, such as the CO_2 reduction reaction (*39*, *71*, *91*) and the oxidation of various chemicals such as methanol (*11*, *13*, *43*).

Stability

High-entropy nanoparticles can potentially provide enhanced stability for catalytic applications, similar to their bulk scale counterparts that feature improved structural stability (*3*, *45*, *53*, *92*). Thermodynamically, the high-entropy nature benefits the formation and stabilization of high-entropy nanoparticles ($\Delta G = \Delta H - T\Delta S$), especially at high temperatures where the $T\Delta S$ term is more pronounced (*20*, *73*, *93*). In situ TEM analysis has revealed the stability of high-entropy alloy and oxide nanoparticles, where the size distribution, particle dispersion, and solid-solution phase remain unchanged even when subjected to temperatures up to 1073 K (*13*, *20*, *73*). Kinetically, the high-entropy mixing may also improve the structural stability because of the size mismatch of the different elements and resultant lattice distortion, which can cause large diffusion barriers that help to prevent phase segregation, particularly at low temperature (*2*, *20*, *53*, *70*). As an example, the diffusion coefficient of Ru atoms in RuRhCoNiIr HEA nanoparticles was simulated to be two orders of magnitude lower compared with the diffusion

of Ru in bimetallic Ru–Ni, suggesting better kinetic stability in HEA nanoparticles (*73*). Another important factor affecting catalyst stability is the interfacial bonding between catalysts and supports to avoid particle aggregation. The high-temperature shock syntheses can enable better interfacial stability between the high-entropy nanoparticles and substrates (*76*, *87*, *94*). Experimentally, the stability of high-entropy catalysts has been illustrated by their steady performance in both high-temperature and electrochemical catalytic reactions (*11*–*13*, *15*, *20*, *36*–*38*, *43*, *44*, *73*, *75*). However, the entropy stabilization role could become limited and surface reconstruction can easily occur in harsh conditions (*95*–*97*). For example, Shahbazian-Yassar *et al.* performed in situ oxidation of $Fe_{0.28}Co_{0.21}Ni_{0.20}Cu_{0.08}Pt_{0.23}$ HEA nanoparticles and observed surface oxidation of the non-noble elements while the core of the HEA nanoparticles remained stable with a Pt-rich composition (Fig. 4G). Qualitative analysis revealed that the HEA nanoparticles exhibit logarithmic oxidation kinetics, resulting in a stable HEA-core and oxide-shell structure after 40 minutes of exposure in an oxidative environment at 400°C (Fig. 4H). By contrast, pure Co nanoparticles underwent catastrophic oxidation kinetics and oxidized within ~1 min. The surface reconstruction or transformation of high-entropy catalysts is often more evident in electrochemical reactions, in which the entropic stabilization effect is less profound compared with chemical leaching and electrochemical redox. Nevertheless, many studies have reported stable performance of high-entropy nanoparticles in diverse electrochemical conditions, especially compared with their fewer-element counterparts (*12*, *29*, *75*, *86*, *87*).

High-throughput screening

Despite the superior catalytic performances observed in several cases, it remains unknown how to generally develop high-entropy nanoparticles for targeted catalytic reaction schemes. In addition, identifying catalytic active sites in high-entropy nanoparticles is challenging because of the complex microstructure and binding energy distribution pattern (*40*, *42*, *98*). These issues may be resolved by taking advantage of emerging high-throughput (*64*, *99*, *100*) and data-driven material discovery approaches (*27*, *71*, *101*–*103*).

Computationally, first-principles-based methods have been developed to predict the composition-structure-property relationships of high-entropy nanoparticles (*84*, *100*, *104*). Additionally, high-throughput computation has been demonstrated for phase prediction of multielemental compositions by following empirical rules derived from high-entropy materials (*46*, *73*) or using calculation of phase diagram (CALPHAD) methods with largely reduced parameter spaces (*105*), both of which are capable of screening millions of elemental compositions (Fig. 5A). However, these calculations are mostly based on thermodynamic equilibrium considerations of bulk materials, which may not be readily transferable to high-entropy nanoparticles because of their small size and synthesis under nonequilibrium conditions.

For the prediction of functional properties (e.g., catalysis) of high-entropy nanoparticles, there are additional challenges, such as building precise atomic packing models and determining binding sites (*11*). Recently, Rossmeisl *et al.* developed a high-throughput computation method combined with supervised learning to explore the random atomic configurations in high-entropy nanoparticles and predict their adsorption energies in catalysis (Fig. 5B) (*27*, *71*, *101*). The authors also simulated the near-continuous binding energy distribution pattern (Fig. 5B) for high-entropy catalysts. On the basis of these calculations, high-performance multielemental catalysts for oxygen reduction and CO_2 reduction were experimentally realized (*27*, *71*, *101*, *106*). Additional machine learning (ML)–based methods are being developed to efficiently explore the configurations of adsorbates on multielemental surfaces, including the effects of variable adsorbate coverage, multiple adsorption species, and surface reconstruction on the catalytic properties (*107*).

Experimentally, researchers have demonstrated the combinatorial synthesis and high-throughput screening of multielemental catalysts (*64*, *108*–*110*). For example, Ludwig *et al.* achieved the combinatorial synthesis of hundreds of high-entropy compositions (~342 per batch) on thin-film substrates using co-sputtering of multiple metal sources, along with high-throughput characterization, including energy-dispersive spectroscopy (composition), XRD (structure), and scanning droplet cell (electrochemistry), to rapidly screen these 2D thin-film samples for rapid catalyst discovery (*64*, *111*–*113*). Direct high-throughput synthesis and screening of high-entropy nanoparticles have also been achieved (*9*, *72*). By combinatorial co-sputtering into ionic liquid (~ 40 μl per cavity, in total 64 cavities), Ludwig *et al.* demonstrated synthesis of CrMnFeCoNi-based HEA nanoparticles immobilized on the microelectrodes with various compositions, which led to the discovery of $Cr_9Mn_{60}Fe_9Co_{11}Ni_{11}$ with exceptional activity for oxygen reduction reaction (*9*). Yao *et al.* reported the high-throughput synthesis of ultrafine and homogeneous HEA nanoparticles with different elemental combinations from binary up to octonary PtPdRhRuIrNiCoFe (Fig. 5C) (*72*). In the process, different metal-precursor solutions were ink printed, followed by a high-temperature radiation shock synthesis to obtain uniform microstructures despite different compositions. Scanning droplet cell screening then enabled the discovery of high-performance PtPdFeCoNi HEA catalysts for oxygen reduction reaction, the catalytic performances of which were verified by conventional rotating disk electrode measurement (*72*). The combinatorial synthesis and high-throughput screening pipeline therefore presents a new paradigm for accelerated exploration of high-entropy nanoparticles.

ML acceleration and active exploration

ML is an excellent tool with which to accelerate materials discovery by enabling extensive prediction of unmeasured compositions (the generalization process in ML), guided exploration to quickly find the performance optima (active learning in ML), and quantitatively understanding of composition and process-structure-property relationships (feature analysis in ML) (*27*, *63*, *71*, *101*–*103*, *114*, *115*). As an example, ML prediction has been used to guide the design of ternary medium-entropy PtFeCu catalysts, illustrating the closed-loop process by (i) model building and simulation data generation, (ii) ML and fitting of the simulation data, (iii) extensive exploration and screening by ML in a larger compositional space, and (iv) experimental verification and feedback to previous simulations and ML models (Fig. 5D) (*116*). A similar process has also been demonstrated for multielemental catalysts in the Ag-Ir-Pd-Pt-Ru space by combining computational prediction with ML and using thin-film–based high-throughput synthesis and screening for data feedback and model refining, thus forming a closed-loop optimization protocol to improve the prediction power toward high-performance catalysts (*63*).

Despite these advances, current efforts can at most cover <1% of available compositions in high-entropy nanoparticles (*113*). Therefore, guided optimization and careful sampling are critical for identifying important data points to save exploration efforts. This can be realized by using active learning methods (e.g., Bayesian optimization and reinforcement learning) (*103*, *117*–*119*). For example, Rossmeisl *et al.* used Bayesian optimization with Gaussian process surrogate function models to discover multielemental catalysts based on computational data (*120*). With ~150 iterations based on Bayesian optimization, many important local optima of targeted properties were discovered, illustrating the great promise of active learning in exploring the vast multidimensional space. Such approaches can also be combined with graph network descriptors of the HEA surfaces and neural networks to accelerate the development of surrogate computational models of the surface and adsorption properties (*107*). Active learning can also enable multiobjective optimization, which has not yet been realized in the development of high-entropy nanoparticles but is highly desirable toward the

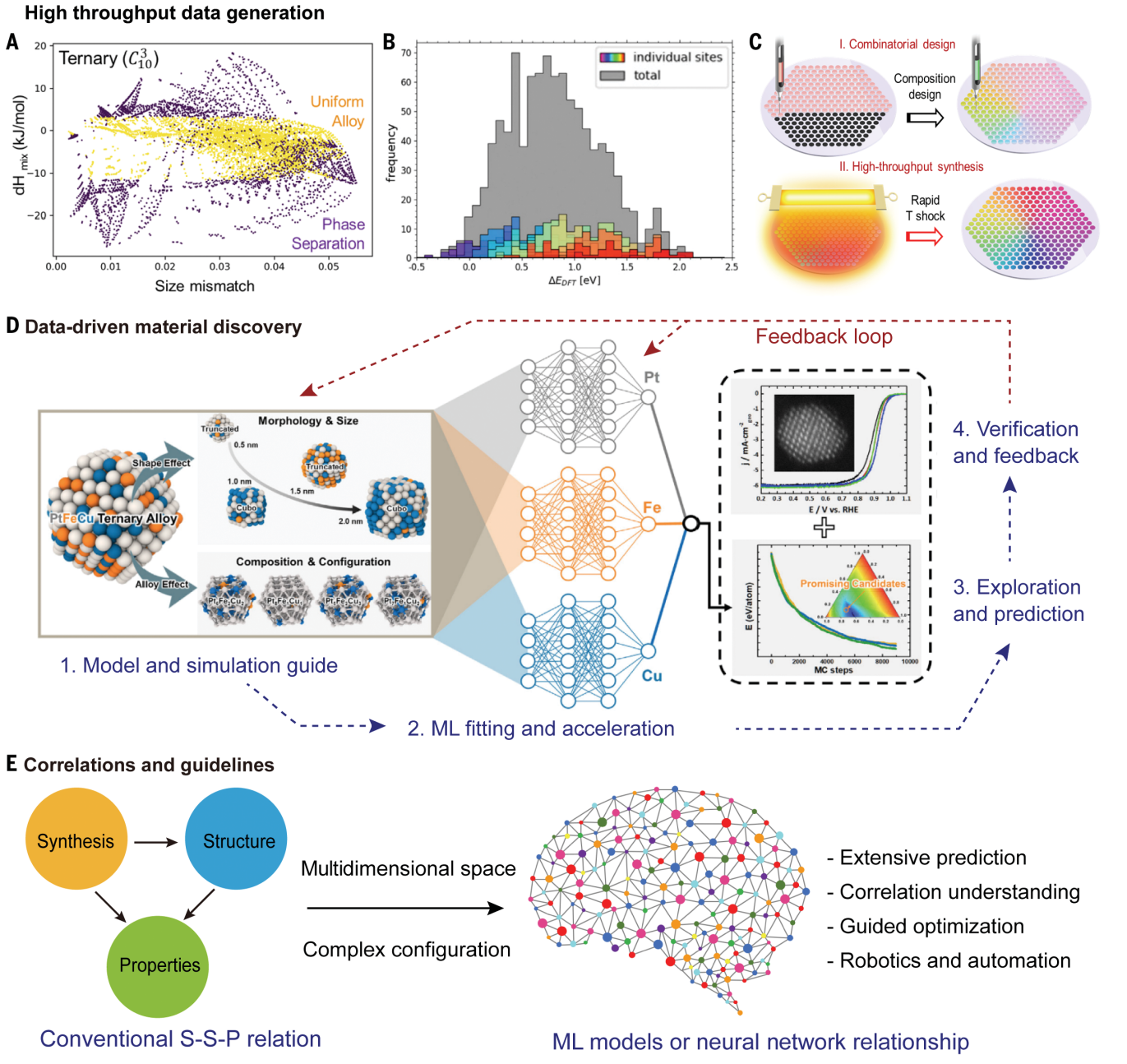

Fig. 5. Data-driven high-entropy nanoparticle discovery. (**A** and **B**) High-throughput computation for structural prediction based on size mismatch and enthalpy (*73*) (A) and adsorption sites and binding energy distribution patterns to predict catalytic properties (B). Reprinted from (*27*) with permission from Elsevier. (**C**) Example of the combinatorial and high-throughput synthesis of high-entropy nanoparticles (*72*). (**D**) Data-driven methodology for the discovery of PtFeCu catalysts consists of (i) modeling and simulation, (ii) ML fitting and acceleration, (iii) composition exploration and prediction, and (iv) experimental verification and feedback. Reprinted from (*116*) with permission from Elsevier. (**E**) Synthesis-structure-property relationships in conventional materials research may be replaced by data-driven approaches featuring ML-trained models for prediction, understanding, and optimization, which could even enable automated discovery.

goal of achieving superior catalysts with simultaneously high activity, selectivity, and stability.

Understanding synthesis-structure-property relationships will always be challenging for material systems as complex as high-entropy nanoparticles. Some initial efforts have used theoretical models and neural networks to decouple the multielemental synergy into ligand effects (i.e., different elements) and coordination effects (i.e., different structures) to correlate the structural features with their catalytic performances (*101*). Therefore, instead of a traditional synthesis-structure-property relationship built upon a clear picture of the catalytic mechanism, data-trained mathematical models may gradually learn and facilitate property prediction, guided optimization, and fundamental understanding of high-entropy nanoparticle catalysts (Fig. 5E). Such trained models (in the form of a Gaussian process model or a neural network) may become a new norm for the study of complex materials such as high-entropy nanoparticles.

Conclusion and outlook

Great progress has been made on high-entropy nanoparticles, but to further advance their

development, continued efforts are needed in many areas, such as synthesis methodologies, advanced characterization, fundamental understanding, and application- and data-driven discoveries, as described below.

Tunable synthesis is currently the most explored aspect of high-entropy nanoparticles and now requires precision. Considering the immiscibility caused by the elemental differences and compositional complexity in high-entropy nanoparticles, syntheses must continue to rely on nonequilibrium approaches in terms of temperature, force, pressure, energy field, etc., to achieve uniform mixing and small particle size. Furthermore, we still need to learn how to balance nonequilibrium syntheses with delicate structural or morphology control in terms of size, phase, shape, facets, and surface decoration, which will require considerable effort and knowledge gained from existing wet chemistry.

An important aspect of high-entropy nanoparticle research that is currently lacking is a fundamental understanding of the surfaces, defects, and elemental distribution in high-entropy nanoparticles, which will have a profound impact on the catalytic properties. We have not yet established basic knowledge of surface or interface elemental segregation, reconstruction, and electronic structure, especially their dynamic evolution under catalytic operation conditions. Integrating state-of-the-art in situ electron microscopies, such as in situ liquid and environmental microscopy, into advanced atomic-resolution chemical analysis and atomic structural imaging will provide valuable insight into the fundamental understanding of active sites and reaction pathways in high-entropy nanomaterials for catalytic applications. Also, we envision the combination of atomic-resolution in situ environmental microscopy with ML-assisted data acquisition and analysis to allow us to capture the critical dynamic changes of high-entropy nanomaterials during catalytic reactions. Information such as the evolution of surface atomic structure, lattice strain, chemical diffusion, and electronic structures of high-entropy nanoparticles will be attained, providing reliable inputs for theoretical calculations and insights into understanding reaction pathways.

High-entropy nanoparticles have great promise for high-performance catalysis and are particularly advantageous for multistep and tandem reactions that require a combination of different active sites. However, it remains an open question how to properly design high-entropy nanoparticles to best fit those reaction schemes. In addition, it is unclear how to identify the active sites and understand the performance origin. Although catalyst discovery based on traditional routes is possible, high-entropy nanoparticle research would greatly benefit from the advancement of high-throughput methodologies and data mining. Currently, combinatorial syntheses and high-throughput screening are mostly limited to thin-film samples and simple electrochemical reactions. Additionally, high-throughput computation often comes at the price of precision for simplicity or computational efficiency, leading to some disparity between screening results and actual trends of performance. Therefore, these data-driven methodologies will likely require the most significant effort in the next stages of research.

Many published research results demonstrate different compositions with interesting properties, but more systematic and standardized reporting is necessary to take full advantage of these "expensive" data (*102*). Therefore, establishing reporting standards for a sharable data repository should be developed so that the knowledge can be better collected and analyzed. Some such efforts are already taking place, such as the establishment of the Materials Data Bank for archiving the 3D atomic coordinates and chemical species of a wide range of materials including multielement and high-entropy nanoparticles determined by AET (*121*). The experimentally determined 3D atomic models of high-entropy nanoparticles can be coupled with computational and ML methods to understand their structure-property relationships at the fundamental level. We expect that with the expanding knowledge of the synthesis-structure-property relationships of high-entropy nanoparticles, an integrated material discovery workflow combining ML-guided optimization and screening will soon become possible to expedite progress in this promising field, particularly multi-objective optimization toward simultaneously high activity, selectivity, stability, and low cost.

REFERENCES AND NOTES

1. J. W. Yeh *et al*., Nanostructured high-entropy alloys with multiple principal elements: Novel alloy design concepts and outcomes. *Adv. Eng. Mater.* **6**, 299–303 (2004). doi: 10.1002/adem.200300567
2. C. M. Rost *et al*., Entropy-stabilized oxides. *Nat. Commun.* **6**, 8485 (2015). doi: 10.1038/ncomms9485; pmid: 26415623
3. E. P. George, D. Raabe, R. O. Ritchie, High-entropy alloys. *Nat. Rev. Mater.* **4**, 515–534 (2019). doi: 10.1038/s41578-019-0121-4
4. B. Niu *et al*., Sol-gel autocombustion synthesis of nanocrystalline high-entropy alloys. *Sci. Rep.* **7**, 3421 (2017). doi: 10.1038/s41598-017-03644-6; pmid: 28611380
5. M. P. Singh, C. Srivastava, Synthesis and electron microscopy of high entropy alloy nanoparticles. *Mater. Lett.* **160**, 419–422 (2015). doi: 10.1016/j.matlet.2015.08.032
6. C.-F. Tsai, P.-W. Wu, P. Lin, C.-G. Chao, K.-Y. Yeh, Sputter deposition of multi-element nanoparticles as electrocatalysts for methanol oxidation. *Jpn. J. Appl. Phys.* **47**, 5755–5761 (2008). doi: 10.1143/JJAP.47.5755
7. P.-C. Chen *et al*., Polyelemental nanoparticle libraries. *Science* **352**, 1565–1569 (2016). doi: 10.1126/science.aaf8402; pmid: 27339985
8. Y. Yao *et al*., Carbothermal shock synthesis of high-entropy-alloy nanoparticles. *Science* **359**, 1489–1494 (2018). doi: 10.1126/science.aan5412; pmid: 29599236
9. T. Löffler *et al*., Discovery of a multinary noble metal-free oxygen reduction catalyst. *Adv. Energy Mater.* **8**, 1802269 (2018). doi: 10.1002/aenm.201802269
10. X. Wang *et al*., Continuous synthesis of hollow high-entropy nanoparticles for energy and catalysis applications. *Adv. Mater.* **32**, e2002853 (2020). doi: 10.1002/adma.202002853; pmid: 33020998
11. H. Li *et al*., Fast site-to-site electron transfer of high-entropy alloy nanocatalyst driving redox electrocatalysis. *Nat. Commun.* **11**, 5437 (2020). doi: 10.1038/s41467-020-19277-9; pmid: 33116124
12. S. Gao *et al*., Synthesis of high-entropy alloy nanoparticles on supports by the fast moving bed pyrolysis. *Nat. Commun.* **11**, 2016 (2020). doi: 10.1038/s41467-020-15934-1; pmid: 32332743
13. J. Feng *et al*., Unconventional alloys confined in nanoparticles: Building blocks for new matter. *Matter* **3**, 1646–1663 (2020). doi: 10.1016/j.matt.2020.07.027
14. Y. Yao *et al*., Extreme mixing in nanoscale transition metal alloys. *Matter* **4**, 2340–2353 (2021). doi: 10.1016/j.matt.2021.04.014
15. M. W. Glasscott *et al*., Electrosynthesis of high-entropy metallic glass nanoparticles for designer, multi-functional electrocatalysis. *Nat. Commun.* **10**, 2650 (2019). doi: 10.1038/s41467-019-10303-z; pmid: 31201304
16. Y. Yang *et al*., Determining the three-dimensional atomic structure of an amorphous solid. *Nature* **592**, 60–64 (2021). doi: 10.1038/s41586-021-03354-0; pmid: 33790443
17. M. Cui *et al*., Multi-principal elemental intermetallic nanoparticles synthesized via a disorder-to-order transition. *Sci. Adv.* **8**, eabm4322 (2022). doi: 10.1126/sciadv.abm4322; pmid: 35089780
18. C.-L. Yang *et al*., Sulfur-anchoring synthesis of platinum intermetallic nanoparticle catalysts for fuel cells. *Science* **374**, 459–464 (2021). doi: 10.1126/science.abj9980; pmid: 34672731
19. T. Wang, H. Chen, Z. Yang, J. Liang, S. Dai, High-entropy perovskite fluorides: A new platform for oxygen evolution catalysis. *J. Am. Chem. Soc.* **142**, 4550–4554 (2020). doi: 10.1021/jacs.9b12377; pmid: 32105461
20. T. Li *et al*., Denary oxide nanoparticles as highly stable catalysts for methane combustion. *Nat. Catal.* **4**, 62–70 (2021). doi: 10.1038/s41929-020-00554-1
21. C. R. McCormick, R. E. Schaak, Simultaneous multication exchange pathway to high-entropy metal sulfide nanoparticles. *J. Am. Chem. Soc.* **143**, 1017–1023 (2021). doi: 10.1021/jacs.0c11384; pmid: 33405919
22. M. Cui *et al*., High-entropy metal sulfide nanoparticles promise high-performance oxygen evolution reaction. *Adv. Energy Mater.* **2002887**, 1–8 (2020).
23. Z. Du *et al*., High-entropy atomic layers of transition-metal carbides (MXenes). *Adv. Mater.* **33**, e2101473 (2021). doi: 10.1002/adma.202101473; pmid: 34365658
24. S. K. Nemani *et al*., High-Entropy 2D Carbide MXenes: $TiVNbMoC_3$ and $TiVCrMoC_3$. *ACS Nano* **15**, 12815–12825 (2021). doi: 10.1021/acsnano.1c02775; pmid: 34128649
25. Q. Dong *et al*., Rapid synthesis of high-entropy oxide microparticles. *Small* **2104761**, e2104761 (2022). doi: 10.1002/smll.202104761; pmid: 35049145
26. T. Ying *et al*., High-entropy van der Waals materials formed from mixed metal dichalcogenides, halides, and phosphorus trisulfides. *J. Am. Chem. Soc.* **143**, 7042–7049 (2021). doi: 10.1021/jacs.1c01580; pmid: 33926192
27. T. A. A. Batchelor *et al*., High-entropy alloys as a discovery platform for electrocatalysis. *Joule* **3**, 834–845 (2019). doi: 10.1016/j.joule.2018.12.015
28. T. Löffler *et al*., Toward a paradigm shift in electrocatalysis using complex solid solution nanoparticles. *ACS Energy Lett.* **4**, 1206–1214 (2019). doi: 10.1021/acsenergylett.9b00531
29. A. Amiri, R. Shahbazian-Yassar, Recent progress of high-entropy materials for energy storage and conversion. *J. Mater. Chem. A Mater. Energy Sustain.* **9**, 782–823 (2021). doi: 10.1039/D0TA09578H
30. Y. Sun, S. Dai, High-entropy materials for catalysis: A new frontier. *Sci. Adv.* **7**, eabg1600 (2021). doi: 10.1126/sciadv.abg1600; pmid: 33980494
31. Y. Chen *et al*., Opportunities for high-entropy materials in rechargeable batteries. *ACS Mater. Lett.* **3**, 160–170 (2021). doi: 10.1021/acsmaterialslett.0c00484
32. Y. Ma *et al*., High-entropy energy materials: Challenges and new opportunities. *Energy Environ. Sci.* **14**, 2883–2905 (2021). doi: 10.1039/D1EE00505G
33. K. Kusada, D. Wu, H. Kitagawa, New aspects of platinum group metal-based solid-solution alloy nanoparticles: Binary to high-entropy alloys. *Chemistry* **26**, 5105–5130 (2020). doi: 10.1002/chem.201903928; pmid: 31863514
34. W.-T. Koo, J. E. Millstone, P. S. Weiss, I.-D. Kim, The design and science of polyelemental nanoparticles. *ACS Nano* **14**,

6407–6413 (2020). doi: 10.1021/acsnano.0c03993; pmid: 32469489

35. B. Jiang *et al*., High-entropy-stabilized chalcogenides with high thermoelectric performance. *Science* **371**, 830–834 (2021). doi: 10.1126/science.abe1292; pmid: 33602853
36. P. Xie *et al*., Highly efficient decomposition of ammonia using high-entropy alloy catalysts. *Nat. Commun.* **10**, 4011 (2019). doi: 10.1038/s41467-019-11848-9; pmid: 31488814
37. H. J. Qiu *et al*., Nanoporous high-entropy alloys for highly stable and efficient catalysts. *J. Mater. Chem. A Mater. Energy Sustain.* **7**, 6499–6506 (2019). doi: 10.1039/C9TA00505F
38. D. Zhang *et al*., Multi-site electrocatalysts boost pH-universal nitrogen reduction by high-entropy alloys. *Adv. Funct. Mater.* **31**, 2006939 (2021). doi: 10.1002/adfm.202006939
39. C. Yang *et al*., Overcoming immiscibility toward bimetallic catalyst library. *Sci. Adv.* **6**, eaaz6844 (2020). doi: 10.1126/sciadv.aaz6844; pmid: 32494647
40. T. Löffler, A. Ludwig, J. Rossmeisl, W. Schuhmann, What makes high-entropy alloys exceptional electrocatalysts? *Angew. Chem. Int. Ed.* **60**, 26894–26903 (2021). doi: 10.1002/anie.202109212; pmid: 34436810
41. Y. Wang, X. Zheng, D. Wang, Design concept for electrocatalysts. *Nano Res.* **15**, 1730–1752 (2021). doi: 10.1007/s12274-021-3794-0
42. T. Löffler *et al*., Comparing the activity of complex solid solution electrocatalysts using inflection points of voltammetric activity curves as activity descriptors. *ACS Catal.* **11**, 1014–1023 (2021). doi: 10.1021/acscatal.0c03313
43. D. Wu *et al*., Platinum-group-metal high-entropy-alloy nanoparticles. *J. Am. Chem. Soc.* **142**, 13833–13838 (2020). doi: 10.1021/jacs.0c04807; pmid: 32786816
44. M. Wu *et al*., Hierarchical polyelemental nanoparticles as bifunctional catalysts for oxygen evolution and reduction reactions. *Adv. Energy Mater.* **10**, 2001119 (2020). doi: 10.1002/aenm.202001119
45. D. B. Miracle, O. N. Senkov, A critical review of high entropy alloys and related concepts. *Acta Mater.* **122**, 448–511 (2017). doi: 10.1016/j.actamat.2016.08.081
46. M. C. Troparevsky, J. R. Morris, P. R. C. Kent, A. R. Lupini, G. M. Stocks, Criteria for predicting the formation of single-phase high-entropy alloys. *Phys. Rev. X* **5**, 011041 (2015). doi: 10.1103/PhysRevX.5.011041
47. R. Guo *et al*., Enthalpy induced phase partition toward hierarchical, nanostructured high-entropy alloys. *Nano Res.* (2021). doi: 10.1007/s12274-021-3912-z
48. P.-C. Chen *et al*., Interface and heterostructure design in polyelemental nanoparticles. *Science* **363**, 959–964 (2019). doi: 10.1126/science.aav4302; pmid: 30819959
49. S. G. Kwon *et al*., Heterogeneous nucleation and shape transformation of multicomponent metallic nanostructures. *Nat. Mater.* **14**, 215–223 (2015). doi: 10.1038/nmat4115; pmid: 25362354
50. Y. Chen *et al*., Ultra-fast self-assembly and stabilization of reactive nanoparticles in reduced graphene oxide films. *Nat. Commun.* **7**, 12332 (2016). doi: 10.1038/ncomms12332; pmid: 27515900
51. L. Hu, Y. Chen, Y. Yao, "Nanoparticles and systems and methods for synthesizing nanoparticles through thermal shock," US Patent Application 20180369771 (2018).
52. Y. Yao, L. Hu, "Thermal shock synthesis of multielement nanoparticles," US Patent Application 11193191B2 (2021).
53. S. A. Kube, J. Schroers, Metastability in high entropy alloys. *Scr. Mater.* **186**, 392–400 (2020). doi: 10.1016/j.scriptamat.2020.05.049
54. M. T. Aronhime, J. K. Gillham, Time-temperature-transformation (Ttt) cure diagram of thermosetting polymeric systems. *Adv. Polym. Sci.* **78**, 83–113 (1986). doi: 10.1007/BFb0035358
55. F. Chen *et al*., High-temperature atomic mixing toward well-dispersed bimetallic electrocatalysts. *Adv. Energy Mater.* **8**, 1800466 (2018). doi: 10.1002/aenm.201800466
56. Y. Yao *et al*., Ultrafast, controllable synthesis of sub-nano metallic clusters through defect engineering. *ACS Appl. Mater. Interfaces* **11**, 29773–29779 (2019). doi: 10.1021/acsami.9b07198; pmid: 31356053
57. Y. Yao *et al*., High temperature shockwave stabilized single atoms. *Nat. Nanotechnol.* **14**, 851–857 (2019). doi: 10.1038/s41565-019-0518-7; pmid: 31406363
58. Y. Zhou *et al*., Tuning the high-temperature wetting behavior of metals toward ultrafine nanoparticles. *Angew. Chem. Int. Ed.* **57**, 2625–2629 (2018). doi: 10.1002/anie.201712202; pmid: 29346707
59. Y. Chen *et al*., Synthesis of monodisperse high entropy alloy nanocatalysts from core@shell nanoparticles. *Nanoscale Horiz.* **6**, 231–237 (2021). doi: 10.1039/D0NH00656D; pmid: 33480921
60. Y. Yang *et al*., Aerosol synthesis of high entropy alloy nanoparticles. *Langmuir* **36**, 1985–1992 (2020). doi: 10.1021/acs.langmuir.9b03392; pmid: 32045255
61. K. Mori *et al*., Hydrogen spillover-driven synthesis of high-entropy alloy nanoparticles as a robust catalyst for CO_2 hydrogenation. *Nat. Commun.* **12**, 3884 (2021). doi: 10.1038/s41467-021-24228-z; pmid: 34162865
62. T. Löffler *et al*., design of complex solid-solution electrocatalysts by correlating configuration, adsorption energy distribution patterns, and activity curves. *Angew. Chem. Int. Ed.* **59**, 5844–5850 (2020). doi: 10.1002/anie.201914666; pmid: 31867829
63. T. A. A. Batchelor *et al*., Complex-solid-solution electrocatalyst discovery by computational prediction and high-throughput experimentation. *Angew. Chem. Int. Ed.* **60**, 6932–6937 (2021). doi: 10.1002/anie.202014374; pmid: 33372334
64. A. Ludwig, Discovery of new materials using combinatorial synthesis and high-throughput characterization of thin-film materials libraries combined with computational methods. *npj Comput. Mater.* **5**, 70 (2019). doi: 10.1038/s41524-019-0205-0
65. F. Waag *et al*., Kinetically-controlled laser-synthesis of colloidal high-entropy alloy nanoparticles. *RSC Advances* **9**, 18547–18558 (2019). doi: 10.1039/C9RA03254A
66. H. Qiao *et al*., Scalable synthesis of high entropy alloy nanoparticles by microwave heating. *ACS Nano* **15**, 14928–14937 (2021). doi: 10.1021/acsnano.1c05113; pmid: 34423972
67. Y. Yao, Q. Dong, L. Hu, Overcoming immiscibility via a milliseconds-long "shock" synthesis toward alloyed nanoparticles. *Matter* **1**, 1451–1453 (2019). doi: 10.1016/j.matt.2019.11.006
68. X. Wang *et al*., Continuous 2000 K droplet-to-particle synthesis. *Mater. Today* **35**, 106–114 (2020). doi: 10.1016/j.mattod.2019.11.004
69. M. Jiao *et al*., Fly-through synthesis of nanoparticles on textile and paper substrates. *Nanoscale* **11**, 6174–6181 (2019). doi: 10.1039/C8NR10137J; pmid: 30874268
70. H. Xu *et al*., Entropy-stabilized single-atom Pd catalysts via high-entropy fluorite oxide supports. *Nat. Commun.* **11**, 3908 (2020). doi: 10.1038/s41467-020-17738-9; pmid: 32764539
71. J. K. Pedersen, T. A. A. Batchelor, A. Bagger, J. Rossmeisl, High-entropy alloys as catalysts for the CO_2 and CO reduction reactions. *ACS Catal.* **10**, 2169–2176 (2020). doi: 10.1021/acscatal.9b04343
72. Y. Yao *et al*., High-throughput, combinatorial synthesis of multimetallic nanoclusters. *Proc. Natl. Acad. Sci. U.S.A.* **117**, 6316–6322 (2020). doi: 10.1073/pnas.1903721117; pmid: 32156723
73. Y. Yao *et al*., Computationally aided, entropy-driven synthesis of highly efficient and durable multi-elemental alloy catalysts. *Sci. Adv.* **6**, eaaz0510 (2020). doi: 10.1126/sciadv.aaz0510; pmid: 32201728
74. D. Morris *et al*., Composition-dependent structure and properties of 5- and 15-element high-entropy alloy nanoparticles. *Cell Rep. Phys. Sci.* **2**, 100641 (2021). doi: 10.1016/j.xcrp.2021.100641
75. D. Wu *et al*., On the electronic structure and hydrogen evolution reaction activity of platinum group metal-based high-entropy-alloy nanoparticles. *Chem. Sci.* **11**, 12731–12736 (2020). doi: 10.1039/D0SC02351E; pmid: 34094468
76. Z. Huang *et al*., Direct observation of the formation and stabilization of metallic nanoparticles on carbon supports. *Nat. Commun.* **11**, 6373 (2020). doi: 10.1038/s41467-020-20084-5; pmid: 33311508
77. Q. Ding *et al*., Tuning element distribution, structure and properties by composition in high-entropy alloys. *Nature* **574**, 223–227 (2019). doi: 10.1038/s41586-019-1617-1; pmid: 31597974
78. B. H. Savitzky *et al*., py4DSTEM: Open source software for 4D-STEM data analysis. *Microsc. Microanal.* **25** (S2), 124–125 (2019). doi: 10.1017/S1431927619001351
79. J. Miao, P. Ercius, S. J. L. Billinge, Atomic electron tomography: 3D structures without crystals. *Science* **353**, aaf2157 (2016). doi: 10.1126/science.aaf2157; pmid: 27708010
80. Y. Yang *et al*., Deciphering chemical order/disorder and material properties at the single-atom level. *Nature* **542**, 75–79 (2017). doi: 10.1038/nature21042; pmid: 28150758
81. J. Zhou *et al*., Observing crystal nucleation in four dimensions using atomic electron tomography. *Nature* **570**, 500–503 (2019). doi: 10.1038/s41586-019-1317-x; pmid: 31243385
82. D. B. Miracle, A structural model for metallic glasses. *Nat. Mater.* **3**, 697–702 (2004). doi: 10.1038/nmat1219; pmid: 15378050
83. J. Pérez-Ramírez, N. López, Strategies to break linear scaling relationships. *Nat. Catal.* **2**, 971–976 (2019). doi: 10.1038/s41929-019-0376-6
84. J. Greeley *et al*., Alloys of platinum and early transition metals as oxygen reduction electrocatalysts. *Nat. Chem.* **1**, 552–556 (2009). doi: 10.1038/nchem.367; pmid: 21378936
85. A. Vojvodic, J. K. Nørskov, New design paradigm for heterogeneous catalysts. *Natl. Sci. Rev.* **2**, 140–143 (2015). doi: 10.1093/nsr/nwv023
86. W.-B. Jung *et al*., Polyelemental nanoparticles as catalysts for a Li-O_2 battery. *ACS Nano* **15**, 4235–4244 (2021). doi: 10.1021/acsnano.0c06528; pmid: 33691412
87. T. Li *et al*., Carbon-supported high-entropy oxide nanoparticles as stable electrocatalysts for oxygen reduction reactions. *Adv. Funct. Mater.* **31**, 2010561 (2021). doi: 10.1002/adfm.202010561
88. E. B. Tetteh *et al*., Zooming-in – Visualization of active site heterogeneity in high entropy alloy electrocatalysts using scanning electrochemical cell microscopy. *Electrochem. Sci. Adv.* •••, 2100105 (2021). doi: 10.1002/elsa.202100105
89. J. Greeley, Theoretical heterogeneous catalysis: Scaling relationships and computational catalyst design. *Annu. Rev. Chem. Biomol. Eng.* **7**, 605–635 (2016). doi: 10.1146/annurev-chembioeng-080615-034413; pmid: 27088666
90. A. Kulkarni, S. Siahrostami, A. Patel, J. K. Nørskov, Understanding catalytic activity trends in the oxygen reduction reaction. *Chem. Rev.* **118**, 2302–2312 (2018). doi: 10.1021/acs.chemrev.7b00488; pmid: 29405702
91. J. Cavin *et al*., 2D high-entropy transition metal dichalcogenides for carbon dioxide electrocatalysis. *Adv. Mater.* **33**, e2100347 (2021). doi: 10.1002/adma.202100347; pmid: 34173281
92. Z. Lei *et al*., Development of advanced materials via entropy engineering. *Scr. Mater.* **165**, 164–169 (2019). doi: 10.1016/j.scriptamat.2019.02.015
93. S. Nie *et al*., Entropy-driven chemistry reveals highly stable denary MgAl2O4-type catalysts. *Chem Catal.* **1**, 648–662 (2021). doi: 10.1016/j.checat.2021.04.001
94. T. Li *et al*., Interface engineering between multi-elemental alloy nanoparticles and a carbon support toward stable catalysts. *Adv. Mater.* **34**, e2106436 (2022). doi: 10.1002/adma.202106436; pmid: 34875115
95. Y. J. Li, A. Savan, A. Kostka, H. S. Stein, A. Ludwig, Accelerated atomic-scale exploration of phase evolution in compositionally complex materials. *Mater. Horiz.* **5**, 86–92 (2018). doi: 10.1039/C7MH00486A
96. Y. J. Li, A. Kostka, A. Savan, A. Ludwig, Atomic-scale investigation of fast oxidation kinetics of nanocrystalline CrMnFeCoNi thin films. *J. Alloys Compd.* **766**, 1080–1085 (2018). doi: 10.1016/j.jallcom.2018.07.048
97. B. Song *et al*., In situ oxidation studies of high-entropy alloy nanoparticles. *ACS Nano* **14**, 15131–15143 (2020). doi: 10.1021/acsnano.0c05250; pmid: 33079522
98. P. Majumdar, J. Greeley, Generalized scaling relationships on transition metals: Influence of adsorbate-coadsorbate interactions. *Phys. Rev. Mater.* **2**, 045801 (2018). doi: 10.1103/PhysRevMaterials.2.045801
99. A. Jain, Y. Shin, K. A. Persson, Computational predictions of energy materials using density functional theory. *Nat. Rev. Mater.* **1**, 15004 (2016). doi: 10.1038/natrevmats.2015.4
100. J. K. Nørskov, T. Bligaard, J. Rossmeisl, C. H. Christensen, Towards the computational design of solid catalysts. *Nat. Chem.* **1**, 37–46 (2009). doi: 10.1038/nchem.121; pmid: 21378799
101. Z. Lu, Z. W. Chen, C. V. Singh, Neural network-assisted development of high-entropy alloy catalysts: Decoupling ligand and coordination effects. *Matter* **3**, 1318–1333 (2020). doi: 10.1016/j.matt.2020.07.029
102. M. Aykol, P. Herring, A. Anapolsky, Machine learning for continuous innovation in battery technologies. *Nat. Rev. Mater.* **5**, 725–727 (2020). doi: 10.1038/s41578-020-0216-y
103. P. M. Attia *et al*., Closed-loop optimization of fast-charging protocols for batteries with machine learning. *Nature* **578**, 397–402 (2020). doi: 10.1038/s41586-020-1994-5; pmid: 32076218
104. S. Curtarolo *et al*., AFLOWLIB.ORG: A distributed materials properties repository from high-throughput ab initio calculations. *Comput. Mater. Sci.* **58**, 227–235 (2012). doi: 10.1016/j.commatsci.2012.02.002
105. O. N. Senkov, J. D. Miller, D. B. Miracle, C. Woodward, Accelerated exploration of multi-principal element alloys

with solid solution phases. *Nat. Commun.* **6**, 6529 (2015). doi: 10.1038/ncomms7529; pmid: 25739749
106. S. Nellaiappan *et al.*, High-entropy alloys as catalysts for the CO_2 and CO reduction reactions: Experimental realization. *ACS Catal.* **10**, 3658–3663 (2020). doi: 10.1021/acscatal.9b04302
107. S. Deshpande, T. Maxson, J. Greeley, Graph theory approach to determine configurations of multidentate and high coverage adsorbates for heterogeneous catalysis. *npj Comput. Mater.* **6**, 1–6 (2020).
108. E. J. Kluender *et al.*, Catalyst discovery through megalibraries of nanomaterials. *Proc. Natl. Acad. Sci. U.S.A.* **116**, 40–45 (2019). doi: 10.1073/pnas.18153581163055920l
109. X. Liu *et al.*, Inkjet printing assisted synthesis of multicomponent mesoporous metal oxides for ultrafast catalyst exploration. *Nano Lett.* **12**, 5733–5739 (2012). doi: 10.1021/nl302992q; pmid: 23051615
110. J. Li *et al.*, Combinatorial screening of Pd-based quaternary electrocatalysts for oxygen reduction reaction in alkaline media. *J. Mater. Chem. A Mater. Energy Sustain.* **5**, 67–72 (2017). doi: 10.1039/C6TA08088J
111. L. Banko *et al.*, Unravelling composition–activity–stability trends in high entropy alloy electrocatalysts by using a data-guided combinatorial synthesis strategy and computational modeling. *Adv. Energy Mater.* **12**, 2103312 (2022). doi: 10.1002/aenm.202103312
112. O. A. Krysiak *et al.*, Searching novel complex solid solution electrocatalysts in unconventional element combinations. *Nano Res.* (2021). doi: 10.1007/s12274-021-3637-z
113. L. Banko, O. A. Krysiak, B. Xiao, T. Löffler, A. Savan, J. K. Pedersen, J. Rossmeisl, W. Schuhmann, A. Ludwig, Combinatorial materials discovery strategy for high entropy alloy electrocatalysts using deposition source permutations. arXiv:2106.08776 [cond-mat.mtrl-sci] (2021).
114. Z. Zhou *et al.*, Machine learning guided appraisal and exploration of phase design for high entropy alloys. *npj Comput. Mater.* **5**, 128 (2019). doi: 10.1038/s41524-019-0265-1
115. H. S. Stein, D. Guevarra, P. F. Newhouse, E. Soedarmadji, J. M. Gregoire, Machine learning of optical properties of materials - predicting spectra from images and images from spectra. *Chem. Sci.* **10**, 47–55 (2018). doi: 10.1039/C8SC03077D; pmid: 30746072
116. H. Chun *et al.*, First-principle-data-integrated machine-learning approach for high-throughput searching of ternary electrocatalyst toward oxygen reduction reaction. *Chem Catal.* **1**, 855–869 (2021). doi: 10.1016/j.checat.2021.06.001
117. T. Lookman, P. V. Balachandran, D. Xue, R. Yuan, Active learning in materials science with emphasis on adaptive sampling using uncertainties for targeted design. *npj Comput. Mater.* **5**, 21 (2019). doi: 10.1038/s41524-019-0153-8
118. R. Yuan *et al.*, Accelerated discovery of large electrostrains in $BaTiO_3$-based piezoelectrics using active learning. *Adv. Mater.* **30**, 1702884 (2018). doi: 10.1002/adma.201702884; pmid: 29315814
119. D. Xue *et al.*, Accelerated search for materials with targeted properties by adaptive design. *Nat. Commun.* **7**, 11241 (2016). doi: 10.1038/ncomms11241; pmid: 27079901
120. J. K. Pedersen *et al.*, Bayesian optimization of high-entropy alloy compositions for electrocatalytic oxygen reduction. *Angew. Chem. Int. Ed.* **60**, 24144–24152 (2021). doi: 10.1002/anie.202108116; pmid: 34506069
121. J. Miao *et al.*, "Materials Data Bank: A database for archiving 3D atomic coordinates and chemical species of materials" (2022); https://www.materialsdatabank.org.

ACKNOWLEDGMENTS

Funding: L.H. acknowledges support from the National Science Foundation (NSF CMMI-1635221) and the US Department of Energy (DOE), Advanced Research Projects Agency – Energy (ARPA-E). J.L. acknowledges support from the NSF (DMR-2026193 for compositionally complex fluorite–based oxides and DMR-2011967 for interfacial science). J.M. acknowledges support from the DOE, Office of Science, Basic Energy Sciences, Division of Materials Sciences and Engineering, under award no. DE-SC0010378 and by STROBE: A National Science Foundation Science and Technology Center under award no. DMR-1548924. C.W. acknowledges support from the DOE, ARPA-E, and the Petroleum Research Fund (PRF) of the American Chemical Society. G.W. acknowledges support from the US National Science Foundation (NSF DMR grant no. 1905572). J.G., I.K., C.W., and L.H. acknowledge the DOE Office of Science, Office of Basic Energy Sciences (BES), Chemical, Biological, and Geosciences Division, Data Science Initiative grant no. DE-SC0020381. Use of computational resources from the National Energy Research Scientific Computing Center is also acknowledged. M.C. acknowledges support from the DOE, Office of Basic Energy Sciences, under early career award no. ERKCZ55 and the Center for Nanophase Materials Sciences, which is a DOE Office of Science User Facility. **Author contributions:** Y.Y., Q.D., A.B., and L.H. wrote the paper with input from J.L., J.M., M.C., C.W., I.G.K., Z.J.R., J.G., G.W., and A.A. **Competing interests:** The authors declare no competing interests. **Data and materials availability:** References to all data are provided in the manuscript.

10.1126/science.abn3103

Science

High-entropy nanoparticles: Synthesis-structure-property relationships and data-driven discovery

Yonggang YaoQi DongAlexandra BrozenaJian LuoJianwei MiaoMiaofang ChiChao WangIoannis G. KevrekidisZhiyong Jason RenJeffrey GreeleyGuofeng WangAbraham AnapolskyLiangbing Hu

Science, 376 (6589), eabn3103. • DOI: 10.1126/science.abn3103

Diversifying nanoparticles

Multielement nanoparticles are attractive for a variety of applications in catalysis, energy, and other fields. A more diverse range and larger number of elements can be mixed together because of high-entropy mixing states accessed by a number of recently developed techniques. Yao *et al*. review these techniques along with characterization methods, high-throughput screening, and data-driven discovery for targeted applications. The wide range of different elements that can be mixed together presents a large number of opportunities and challenges. —BG

Science (ISSN) is published by the American Association for the Advancement of Science. 1200 New York Avenue NW, Washington, DC 20005. The title *Science* is a registered trademark of AAAS.